Electronic supporting information (ESI)

Ni-foam-structured MoNi$_4$-MoO$_x$ nanocomposite catalyst for hydrogenation of dimethyl oxalate to ethanol

Jian Zhu, Weidong Sun, Song Wang, Guofeng Zhao, Ye Liu, Yong Lu*

Shanghai Key Laboratory of Green Chemistry and Chemical Processes, East China Normal

University, Shanghai 200062, China.

Fax: (+86) 21-62233424, E-mail: ylu@chem.ecnu.edu.cn

Materials and Methods

Catalyst preparation

Synthesis of the MoNi$_4$-MoO$_x$/Ni-foam catalyst

Firstly, the NiMoO$_4$·xH$_2$O/Ni-foam substrates were prepared by a facile hydrothermal method. Before hydrothermal treatment, the circular Ni-foam chips (1.5 mm thick, 8.0 mm diameter, 100 pores per inch (PPI); purchased from Suzhou Taili Material Co., Ltd) were carefully cleaned with 0.1 mol L^{-1} HCl solution in an ultrasound bath for 20 min at room temperature to remove the surface nickel oxide and then washed thoroughly with deionized water. As-cleaned Ni-foam chips were transferred into a 120 mL Teflon-lined stainless steel autoclave filled with 80 mL mixture aqueous solution of 20 mmol L^{-1} Ni(NO$_3$)$_2$·6H$_2$O (99 wt% purity, Aldrich) and 10 mmol L^{-1} (NH$_4$)$_6$Mo$_7$O$_{24}$ (99 wt% purity, Aldrich). The reactant system was heated to 140 ^{o}C and kept for 9 hours. After cooling down to room temperature naturally, the Ni-foams coated with golden NiMoO$_4$·xH$_2$O crystals were rinsed thoroughly by using deionized water and dried in air at 100 °C for 12 h. Finally, the as-obtained NiMoO$_4$·xH$_2$O/Ni-foam substrates were calcined in air at 350 ^{o}C for 2 h followed by reduced in H$_2$ at target temperature (350-500 ^{o}C) for 2 h to form the catalyst products that are denoted as MoNi$_4$-MoO$_x$/Ni-foam-m, where m stand for reduction temperature (°C).

Synthesis of the model catalyst of MoNi$_4$/SiO$_2$

The MoNi$_4$/SiO$_2$ catalyst was prepared by an incipient wetness impregnation method. Typically, the SiO$_2$ (1.0 g, Aldrich) was firstly impregnated with 5 ml aqueous solution containing 1.49 g Ni(NO$_3$)$_2$·6H$_2$O, and dried at 100 ^{o}C for 12 h. Then, the obtained samples were impregnated with 1

ml aqueous solution containing 0.23 g $(NH_4)_6Mo_7O_{24}$ followed by dried at 100 °C for 12 h and calcined in air at 450 °C for 2 h. Finally, the as-obtained precursors were reduced in H_2 at 700 °C for 2 h to form the $MoNi_4/SiO_2$ catalyst. Notably, the initial mole ratios of Ni/Mo was 4.

Synthesis of the model catalyst of MoNi$_4$-MoO$_x$/SiO$_2$

The $MoNi_4$-MoO_x/SiO$_2$ catalyst was prepared by an incipient wetness impregnation method. Typically, the SiO$_2$ (1.0 g) was firstly impregnated with 5 ml aqueous solution containing 1.49 g $Ni(NO_3)_2·6H_2O$, and dried at 100 °C for 12 h. Then, the obtained samples were impregnated with 1 ml aqueous solution containing 0.46 g $(NH_4)_6Mo_7O_{24}$ followed by dried at 100 °C for 12 h and calcined in air at 450 °C for 2 h. Finally, the as-obtained precursors were reduced in H_2 at 500 °C for 2 h to form the $MoNi_4$-MoO_x/SiO$_2$ catalyst. Notably, the initial mole ratios of Ni/Mo was 2.

Synthesis of the model catalyst of MoO$_x$/SiO$_2$

The MoO_x/SiO$_2$ catalyst was prepared by an incipient wetness impregnation method. Typically, the SiO$_2$ (1.0 g) was firstly impregnated with 5 ml aqueous solution containing 0.46 g $(NH_4)_6Mo_7O_{24}$ followed by dried at 100 °C for 12 h and calcined in air at 450 °C for 2 h. Finally, the as-obtained samples were reduced in H_2 at 500 °C for 2 h to form the MoO_x/SiO$_2$ catalyst.

Synthesis of the model catalyst of Ni/SiO$_2$

The Ni/SiO$_2$ catalyst was prepared by an incipient wetness impregnation method. Typically, the SiO$_2$ (1.0 g, Aldrich) was firstly impregnated with 5 ml aqueous solution containing 1.49 g $Ni(NO_3)_2·6H_2O$ followed by dried at 100 °C for 12 h and calcined in air at 450 °C for 2 h. Finally, the as-obtained samples were reduced in H_2 at 400 °C for 2 h to form the Ni/SiO$_2$ catalyst.

Catalyst characterization

X-ray diffraction (XRD) measurement was conducted to analyze the structure and crystallinity of all catalysts. XRD patterns were acquired using a Rigaku Ultra IV diffractometer (Japan), using copper Kα radiation (λ = 0.1542 nm) at 30 kV and 25 mA in the 2θ scanning range of 5-80° at a scanning rate of 20° min^{-1}. Transmission electron microscopy (TEM) images were recorded on a Tecnai G2 F30 high-resolution transmission electron microscope (USA), and before measurement, the samples were uniformly dispersed in ethanol, and then placed onto the copper grids. Scanning electron microscopy (SEM) measurement was performed on a Hitachi S-4800 (Japan) with an accelerating voltage of 3.0 kV. The X-ray photoelectron spectroscopy (XPS) was recorded on an Escalab 250xi spectrometer, using a standard Al Kα X-ray source (300 W) and an analyzer pass energy of 20 eV. All binding energies were referenced to the adventitious C1s line at 284.6 eV. N_2 adsorption-desorption isotherms were measured at -196 °C on a BELSORP-MAX gas adsorption analyzer after the catalysts were degassed under high vacuum at 300 °C for 6 h. Specific surface area (SSA) was determined from N_2 adsorption isotherm using standard Brunauer-Emmett-Teller (BET) theory. The pore size distribution was determined using the Barrett-Jovner-Halenda (BJH) method calculated by the adsorption isotherm.

Reactivity tests

The gas-phase chemoselective hydrogenation of DMO to EtOH was performed in a fixed-bed stainless-steel reactor with 8 mm inner diameter. Briefly, circular catalyst chips of 0.5 g were packed layer by layer into into reactor and activated in a pure H_2 flow at target temperature (350-500 °C) for 2 h. After cooling down to 230 °C and raising the H_2 pressure to 2.5 MPa, the DMO methanol solution (13 wt%) was fed into the catalyst bed reactor by passing through a evaporator

(200 °C). The DMO methanol solution was pumped using high-pressure advection pump and the flow velocity of H_2 was controlled by the calibrated mass flow controller. The liquid effluent was collected using a cold trap (-5 °C) and analyzed on a Shimadzu 2014C gas chromatography-flame ionization detector (GC-FID) with a 30 m HP-INNOWax capillary column (DIMKA). The DMO conversion and products selectivity were calculated based on the following general equations:

$$DMO\ conversion\ (\%)= \left[1-\frac{f_{DMO}A_{DMO,\ out}}{\Sigma f_i A_{i,out} + f_{DMO}A_{DMO,\ out}}\right]\times100\%$$

$$i\ selectivity\ (\%)= \left[\frac{f_i A_{i,\ out}}{\Sigma f_i A_{i,out}}\right]\times100\%$$

where $A_{i,out}$ and f_i are the chromatographic peak area at the outlet and the relative molar calibration factor of the individual product i (i = MG, EG, EtOH, MA, 2-methoxyethanol, 2-ethoxyethanol, propanediol, butanediol, respectively).

Notably, we carried out the kinetic study and used Arrhenius plots to derive apparent activation energies (E_a) for all reactions (including DMO-to-MG, MG-to-EG, EG-to-EtOH, MG-to-MA, and MA-to-EtOH). To obtain the intrinsic activities, apparent activation energy was calculated at low conversion of below 15% by controlling reactant weight hour space velocities.

Tables and Figures

Table S1. Comparison of the representative MoNi$_4$-MoO$_x$/Ni-foam-400 catalyst with the reported catalysts for DMO hydrogenation to EtOH reaction.

Catalyst	Temp. (°C)	n(H$_2$)/ n(DMO)	WHSV (h^{-1})	DMO Conv. (%)	EtOH Sel. (%)	Life span (h)	Ref.
Cu/SiO$_2$	280	200	2.0	100	83	>200	1
Cu@CuPSNTs	280	200	2.0	100	91	>200	2
B-Cu/SiO$_2$	280	200	2.0	100	86	n.a.[a]	3
Cu/Al$_2$O$_3$	270	150	0.3	100	95	<220	4
Cu/ZrO$_2$	270	150	0.3	100	70	>220	4
20Cu80Al	270	200	0.2	100	95	>200	5
Cu/ZrO$_2$/Al$_2$O$_3$	270	150	0.3	100	97	>200	6
Ni-Cu/SiO$_2$	280	200	1.0	100	74	>100	7
Ce-Cu/SiO$_2$	280	200	0.8	100	92	>200	8
Mo$_2$C	200	200	0.2	100	71	>300	9
Fe$_5$C$_2$	260	180	0.2	100	90	>150	10
Cu-Mo$_2$C	200	200	0.2	100	67	>300	11
This work	230	180	0.22	100	93	>220	

[a]Not available (n.a.)

Table S2. Performance of vapor-phase chemoselective hydrogenation of DMO to EtOH over model catalysts.

Catalyst	DMO Conversion (%)	Selectivity (%)			
		EtOH	MG	EG	MA
Ni/SiO$_2$	23.4	0.1	97.8	1.1	1.0
MoNi$_4$/SiO$_2$[a]	99.9	74.3	4.5	1.4	19.8
MoO$_2$/SiO$_2$[a]	33.7	0.5	94.2	2.4	2.9
MoNi$_4$-MoO$_2$/SiO$_2$[a]	99.9	84.4	4.2	1.3	10.1
MoNi$_4$-MoO$_2$/SiO$_2$-M	99.9	79.1	4.1	1.1	15.7
MoNi$_4$-MoO$_3$/SiO$_2$-M	99.9	82.6	3.9	1.1	12.4

Reaction conditions: 230 °C, 2.5 MPa, WHSV$_{DMO}$ of 0.22 h^{-1}, n(H$_2$)/n(DMO) of 180.

Note: [a] the catalysts prepared by incipient wetness impregnation followed by reduction in H$_2$. The MoNi$_4$-MoO$_2$/SiO$_2$-M catalyst was prepared by mechanical mixing method using MoNi$_4$/SiO$_2$ and MoO$_2$/SiO$_2$. [b]The MoNi$_4$-MoO$_3$/SiO$_2$-M catalyst was prepared by mechanical mixing method using MoNi$_4$/SiO$_2$ and MoO$_3$/SiO$_2$.

Table S3. Physicochemical properties of the $MoNi_4$-MoO_x/Ni-foam catalysts reduced at different temperature.

Reduction temp. (^oC)	S_{BET} ($m^2\ g^{-1}$)	V_{pore} ($cm^3\ g^{-1}$)	Mean pore diameter (nm)
350	92	0.062	2.8
400	39	0.037	3.8
450	42	0.041	3.6
500	38	0.036	3.9

Table S4. Surface metal composition of the $MoNi_4$-MoO_x/Ni-foam catalysts by XPS.

Reduction temp. (°C)	Surface metal composition (at.%)				Surface metal ratio (at./at.)		
	Ni^{2+}	Ni^0	Mo^{n+}	Mo^0	Mo^0/Ni^0	Mo^0/Mo^{n+}	$Mo^0/(Mo^{n+}+Mo^0)$
350	14	35	50	1	0.03	0.02	0.02
400	9	43	37	11	0.26	0.30	0.23
450	7	44	34	15	0.34	0.44	0.31
500	6	44	29	21	0.48	0.72	0.42

Note: Mo^{n+} includes Mo^{4+}, Mo^{5+} and Mo^{6+} in MoO_x.

Table S5. Reaction rates of $MoNi_4/SiO_2$ and $MoNi_4\text{-}MoO_x/SiO_2$ for reaction steps involved in DMO-to-EtOH process.

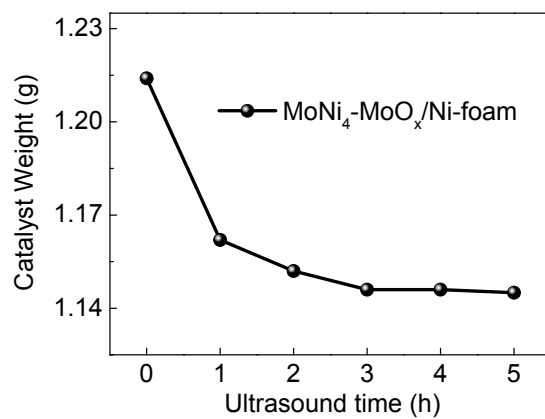| Catalyst	$MoNi_4/SiO_2$	$MoNi_4\text{-}MoO_x/SiO_2$
$WHSV_{DMO}$ (h^{-1})	4.4	4.4
DMO conversion (%)	10.2	10.7
Reaction rate of DMO to MG (mmol g^{-1} h^{-1})	3.8	4.0
$WHSV_{MG}$ (h^{-1})	3.52	3.52
MG conversion (%)	13.7	13.7
EG selectivity (%)	52.4	50.3
MA selectivity (%)	48.6	49.7
Reaction rate of MG to EG (mmol g^{-1} h^{-1})	2.8	2.7
Reaction rate of MG to MA (mmol g^{-1} h^{-1})	2.6	2.7
$WHSV_{EG}$ (h^{-1})	2.64	2.64
EG conversion (%)	5.8	6.2
Reaction rate of EG to EtOH (mmol g^{-1} h^{-1})	2.5	2.6
$WHSV_{MA}$ (h^{-1})	0.88	0.88
MA conversion (%)	2.5	4.6
Reaction rate of MA to EtOH (mmol g^{-1} h^{-1})	0.29	0.55

Fig. S1 Weight loss of the representative MoNi$_4$-MoO$_x$/Ni-foam-400 catalyst against ultrasonic treatment time in methanol.
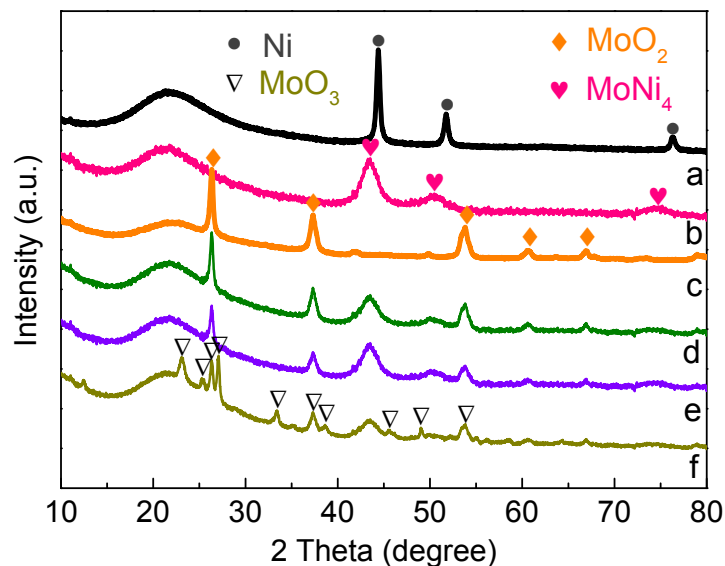
Fig. S2 XRD patterns of used model catalysts of (a) Ni/SiO$_2$, (b) MoNi$_4$/SiO$_2$ (Ni/Mo=4), (c) MoO$_x$/SiO$_2$, (d) MoNi$_4$-MoO$_x$/SiO$_2$ (Ni/Mo=2), (e) MoNi$_4$-MoO$_2$/SiO$_2$-M and (f) MoNi$_4$-MoO$_3$/SiO$_2$-M.

Note: the MoNi$_4$-MoO$_2$/SiO$_2$-M catalyst was prepared by mechanical mixing method using MoNi$_4$/SiO$_2$ and MoO$_2$/SiO$_2$. [b]The MoNi$_4$-MoO$_3$/SiO$_2$-M catalyst was prepared by mechanical mixing method using MoNi$_4$/SiO$_2$ and MoO$_3$/SiO$_2$.
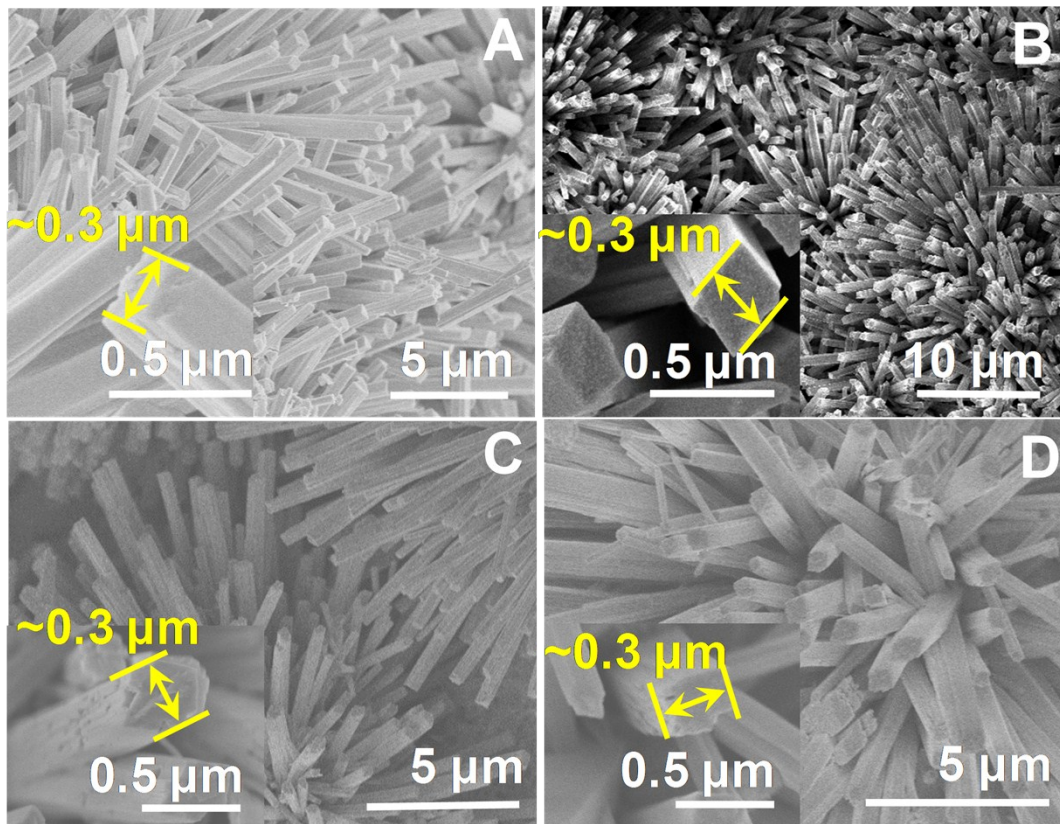
Fig. S3. SEM images of the MoNi$_4$-MoO$_x$/Ni-foam catalysts reduced at 350 ^{o}C (A), 400 ^{o}C (B), 450 ^{o}C (C) and 500 ^{o}C (D).
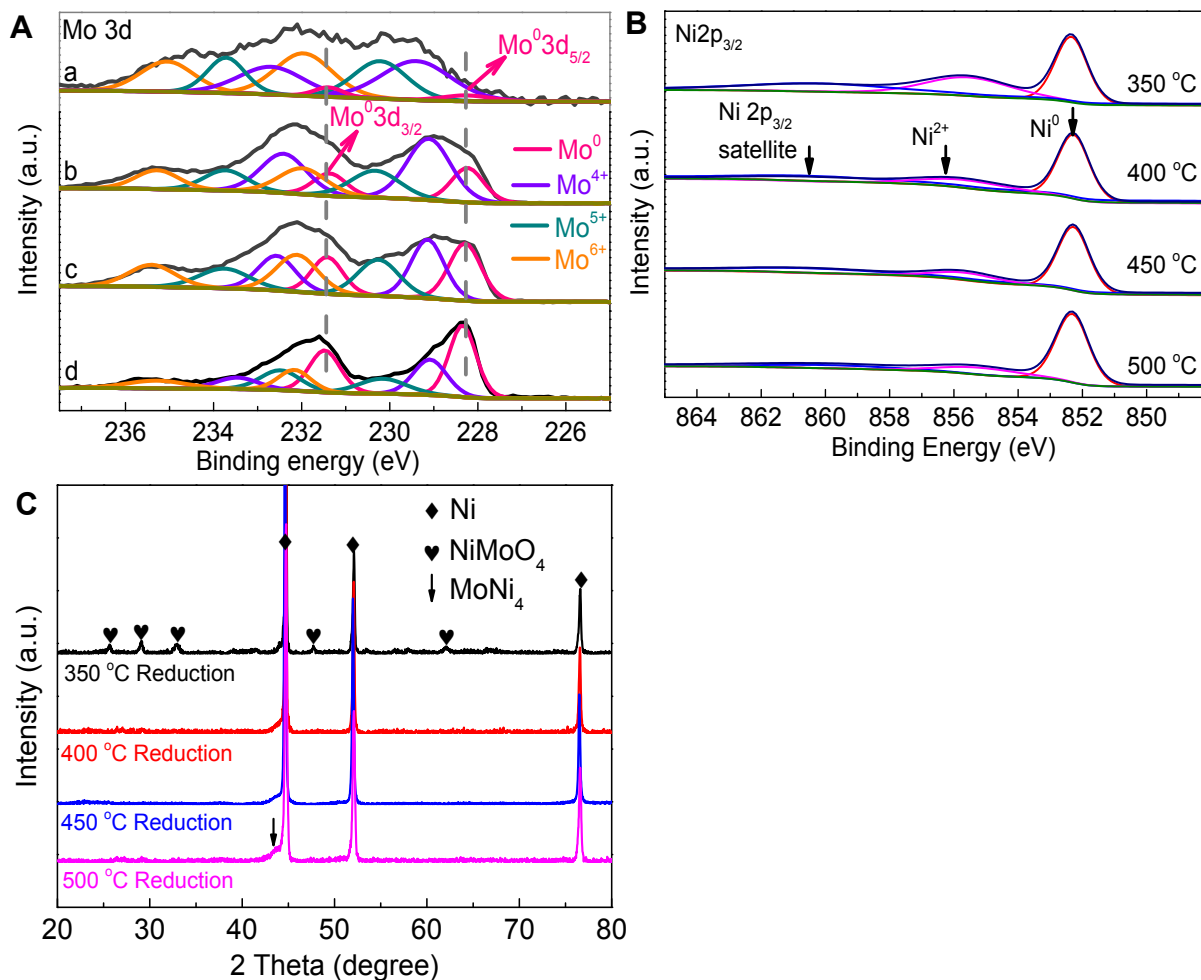
Fig. S4 XPS spectra in Mo3d (A) and Ni2p (B) regions and XRD patterns (C) of the $MoNi_4$-MoO_x/Ni-foam catalysts reduced at varied temperature in H_2.
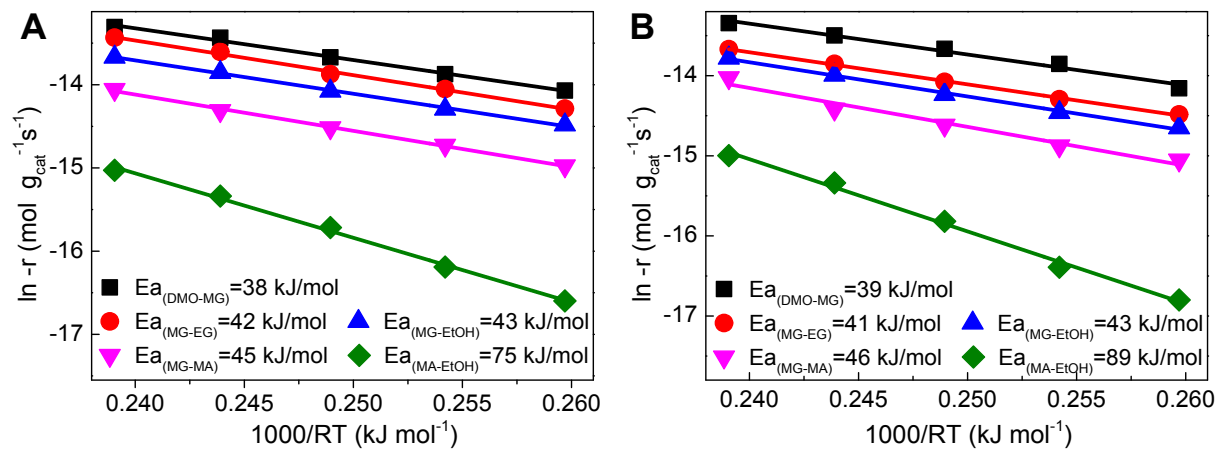
Fig. S5 Activation energies of MoNi$_4$-MoO$_x$/Ni-foam catalysts reduced at (A) 450 ^{o}C and (B) 500 ^{o}C for the reaction steps involved in the DMO-to-EtOH process.

Reference

(1) Gong, J., Yue, H., Zhao, Y., Zhao, S., Zhao, L., Lv, J. Synthesis of Ethanol via Syngas on Cu/SiO$_2$ Catalysts with Balanced Cu^0-Cu$^+$ Sites. *J. Am. Chem. Soc.* **2012**, *134*, 13922-13925.

(2) Yue, H., Zhao, Y., Zhao, S., Ma, X. B., Gong, J. L. A Copper-phyllosilicate Core-Sheath Nanoreactor for Carbon-oxygen Hydrogenolysis Reactions. *Nat. Commun*. **2013,** *4*, 2339-2345.

(3) Zhao, S., Yue, H., Zhao, Y., Wang, B., Geng, Y., Lv, J. Chemoselective Synthesis of Ethanol via Hydrogenation of Dimethyl Oxalate on Cu/SiO$_2$: Enhanced Stability with Boron Dopant. *J. Catal.* **2013**, *297*, 142-150.

(4) Zhu, Y., Ding, G., Zhu, S., Zheng, H., Li, Y. Highly Selective Synthesis of Ethylene Glycol and Ethanol via Hydrogenation of Dimethyl Oxalate on Cu Catalysts: Influence of Support. *Appl. Catal. A* **2013**, *468*, 296-304.

(5) Zhu, Y., Kong, X., Li, X., Ding, G., Li, Y. W. Cu Nanoparticles Inlaid Mesoporous Al$_2$O$_3$ as a High-performance Bifunctional Ccatalyst for Ethanol Synthesis via Dimethyl Oxalate Hydrogenation. *ACS Catal.* **2014**, *4*, 3612-3620.

(6) Zhu, Y., Xiao, K., Zhu, S., Fang, D., Zheng, H. Zhu, Y. Construction of Cu/ZrO$_2$/Al$_2$O$_3$ Composites for Ethanol Synthesis: Synergies of Ternary Sites for Cascade Reaction. *Appl. Catal. B* **2015**, *166*, 551-559.

(7) Zhao, Y., Zhao, S., Geng, Y., Shen, Y., Yue, H., Lv, J. Ni-containing Cu/SiO$_2$ Catalyst for the Chemoselective Synthesis of Ethanol via Hydrogenation of Dimethyl Oxalate. *Catal. Today* **2016**, *276*, 28-35.

(8) Ai, P., Tan, M., Reubroycharoen, P., Wang, Y., Feng, X., Liu, G. Probing the Promotional Roles of Cerium in the Structure and Performance of Cu/SiO_2 Catalysts for Ethanol Production. *Catal. Sci. Technol*. **2018**, *24*, 6441-6451.

(9) Liu, Y., Ding, J., Sun, J., Zhang, J., Bi, J. Liu, K. Molybdenum Carbide as an Efficient Catalyst for Low-temperature Hydrogenation of Dimethyl Oxalate. *Chem. Commun*. **2016**, *52*, 5030-5032.

(10) He, J., Zhao, Y., Wang, Y., Wang, J., Zheng, J. Zhang, H. A Fe_5C_2 Nanocatalyst for the Preferential Synthesis of Ethanol via Dimethyl Oxalate Hydrogenation. *Chem. Commun.* **2017**, *53*, 5376-5379.

(11) Liu, Y., Ding, J., Bi, J., Sun, Y., Zhang, J., Liu, K. Effect of Cu-doping on the Structure and Performance of Molybdenum Carbide Catalyst for Low-temperature Hydrogenation ofDimethyl Oxalate to Ethanol. *Appl. Catal. A* **2017**, *529*, 143-155.